CORRECTED 5 DECEMBER 2024; SEE LAST PAGE

INFLUENZA

A single mutation in bovine influenza H5N1 hemagglutinin switches specificity to human receptors

Ting-Hui Lin[1], Xueyong Zhu[1], Shengyang Wang[2,3], Ding Zhang[1], Ryan McBride[2,3], Wenli Yu[1], Simeon Babarinde[1], James C. Paulson[2,3]*, Ian A. Wilson[1]*

In 2024, several human infections with highly pathogenic clade 2.3.4.4b bovine influenza H5N1 viruses in the United States raised concerns about their capability for bovine-to-human or even human-to-human transmission. In this study, analysis of the hemagglutinin (HA) from the first-reported human-infecting bovine H5N1 virus (A/Texas/37/2024, Texas) revealed avian-type receptor binding preference. Notably, a Gln^{226}Leu substitution switched Texas HA binding specificity to human-type receptors, which was enhanced when combined with an Asn^{224}Lys mutation. Crystal structures of the Texas HA with avian receptor analog LSTa and its Gln^{226}Leu mutant with human receptor analog LSTc elucidated the structural basis for this preferential receptor recognition. These findings highlight the need for continuous surveillance of emerging mutations in avian and bovine clade 2.3.4.4b H5N1 viruses.

Since the first highly pathogenic avian influenza (HPAI) H5N1 virus A/goose/Guangdong/1/1996 emerged in 1996 (*1*), avian H5-subtype viruses have spread widely in Europe, Africa, North America, and Asia through migratory birds, resulting in diverse phylogenetic clades and subclades (*2*–*8*). In late 2021, an H5N1 clade 2.3.4.4b virus was detected in North America (*9*–*12*) and was able to infect a wide spectrum of avian species and mammals, including marine and terrestrial mammals and humans (*13*–*25*). In early 2024, the first human-infecting bovine H5N1 case involving close contact with infected dairy herds was reported in Texas, which heralded the outbreak of HPAI H5N1 virus in dairy cattle in the US Genetic analysis of the influenza hemagglutinin (HA) indicated that this H5N1 virus (A/Texas/37/2024, Texas) belonged to H5 clade 2.3.4.4b (*26*). Since then, this virus has been detected in at least 282 dairy herds in 14 states in the US, with potential interspecies transmission (*27*, *28*), including to farm cats, poultry, and humans.

As of the latest available data in October 2024, the US Centers for Disease Control and Prevention (CDC) has reported 15 human infections worldwide with the 2.3.4.4b virus (*29*) but 17 human infections with the H5 subtype in the US since 2022, including cases of the 2.3.4.4b virus from exposure to infected cows and poultry (*30*). Humans infected from cows and poultry have reported mild conjunctivitis and respiratory symptoms (*26*, *29*, *31*). Historically, however, sporadic human infections from earlier clades of H5N1 from exposure to infected poultry resulted in 30% mortality rates in hospitalized cases (*32*), which is likely an overestimate, as it does not take into account infections that were minor or not reported. Although there are currently no documented cases of transmission between humans, there is concern that the virus could adapt for human-to-human transmission and potentially result in an influenza pandemic.

One barrier for transmission of avian viruses to humans is a mismatch in the receptor specificity of the HA that binds sialic acid receptors (*33*). The HA of avian influenza viruses recognizes "avian-type" receptors with sialic acid in an α2-3 linkage (Neu5Acα2-3Gal). By contrast, the HA of human viruses recognizes "human-type" receptors with sialic acid in an α2-6 linkage (Neu5Acα2-6Gal), which are abundantly expressed in the upper human airway (*34*). Acquisition of human-type receptor specificity is believed to be required for human-to-human transmission of influenza virus and is one of the major factors considered by the CDC for pandemic risk of a novel animal strain (*33*, *35*, *36*).

A switch in receptor binding preference of human viruses from avian or swine virus progenitors was previously shown for influenza pandemics in 1918, 1957, 1968, and 2009, when HA acquired Asp^{190} and Asp^{225} (H3 numbering) in the H1 subtype and Leu^{226} and Ser^{228} in H2 and H3 subtypes (*37*–*39*). In the 1918 and 2009 H1N1 pandemics, there is some evidence for human-transmissible viruses with a single mutation (Glu^{190}Asp), which conferred human-type receptor specificity while retaining avian-type receptor specificity (dual specificity) (*38*, *40*, *41*). The sporadic human infections with the avian H5 subtype have therefore raised global health concerns as to whether H5 viruses could acquire the ability to switch receptor preference. Several studies from the past decade have shown that Gln^{226}Leu and Gly^{228}Ser substitutions in avian H5 HA can promote binding to human receptors, although some binding to avian-type receptors is also retained (*42*–*48*). Aerosol transmission studies in ferrets have showed that additional mutations along with Leu^{226} or Ser^{228} can increase human receptor binding and concomitantly reduce avian-type receptor binding (*49*, *50*). However, none of these mutants showed a complete switch to human receptors.

To assess the potential for the recent 2.3.4.4b viruses to acquire human-type receptor specificity, we introduced mutations into the receptor binding site (RBS) of the Texas HA protein and assessed receptor binding using surface plasmon resonance (SPR), enzyme-linked immunosorbent assay (ELISA), and glycan array analyses. Furthermore, we determined crystal structures for Texas H5 HA and its Gln^{226}Leu mutant with avian and human receptor analogs to provide insights into the molecular basis of H5 HA receptor preference.

Results

Receptor specificity of Texas H5 HA and mutants

To examine glycan binding of the wild-type (WT) bovine Texas H5 HA, we used an SPR assay with extended linear avian-type α2-3 (3SLN$_3$-L) and human-type α2-6 sialosides (6SLN$_3$-L), which contain three N-acetyllactosamine (LacNAc, Galβ1-4GlcNAc) repeats; an ELISA with linear and biantennary N-linked glycan sialosides with multiple LacNAc repeats (1 to 3); and a glycan array assay with a variety of α2-3 and α2-6 sialosides (Figs. 1 and 2 and figs. S1 to S4) (see supplementary materials and table S2). The SPR showed that WT Texas HA exhibits strong binding to α2-3 SLN$_3$, with an apparent dissociation constant (K_D) of 138 nM, whereas no binding to α2-6 SLN$_3$ was detected (K_D >1 mM) (Fig. 1C). This result was consistent with the ELISA assay, which showed binding to linear α2-3 sialosides (3SLN$_{1-3}$), as well as glycan array analysis, where binding was observed to a variety of linear and biantennary α2-3 sialosides (Fig. 1, D and E). In all three assays, the WT Texas H5 HA exhibited strong avian-type specificity, as also reported recently by others (*51*, *52*).

Notably, when we introduced a Gln^{226}Leu substitution, binding specificity was completely switched from avian-type to human-type receptors in SPR, ELISA, and glycan array, with no detectable binding to α2-3 sialosides (Fig. 2). In the ELISA, binding to biantennary N-linked glycan sialosides was stronger than to linear sialosides (Fig. 2B). This observation is also consistent with the glycan array analysis, which showed that the Gln^{226}Leu mutant preferentially binds to α2-6 sialylated biantennary glycans (Fig. 2C and table S2). Although the

[1]Department of Integrative Structural and Computational Biology, The Scripps Research Institute, La Jolla, CA, USA. [2]Department of Molecular Medicine, The Scripps Research Institute, La Jolla, CA, USA. [3]Department of Immunology and Microbiology, The Scripps Research Institute, La Jolla, CA, USA.
*Corresponding author. Email: wilson@scripps.edu (I.A.W.); jpaulson@scripps.edu (J.C.P.)

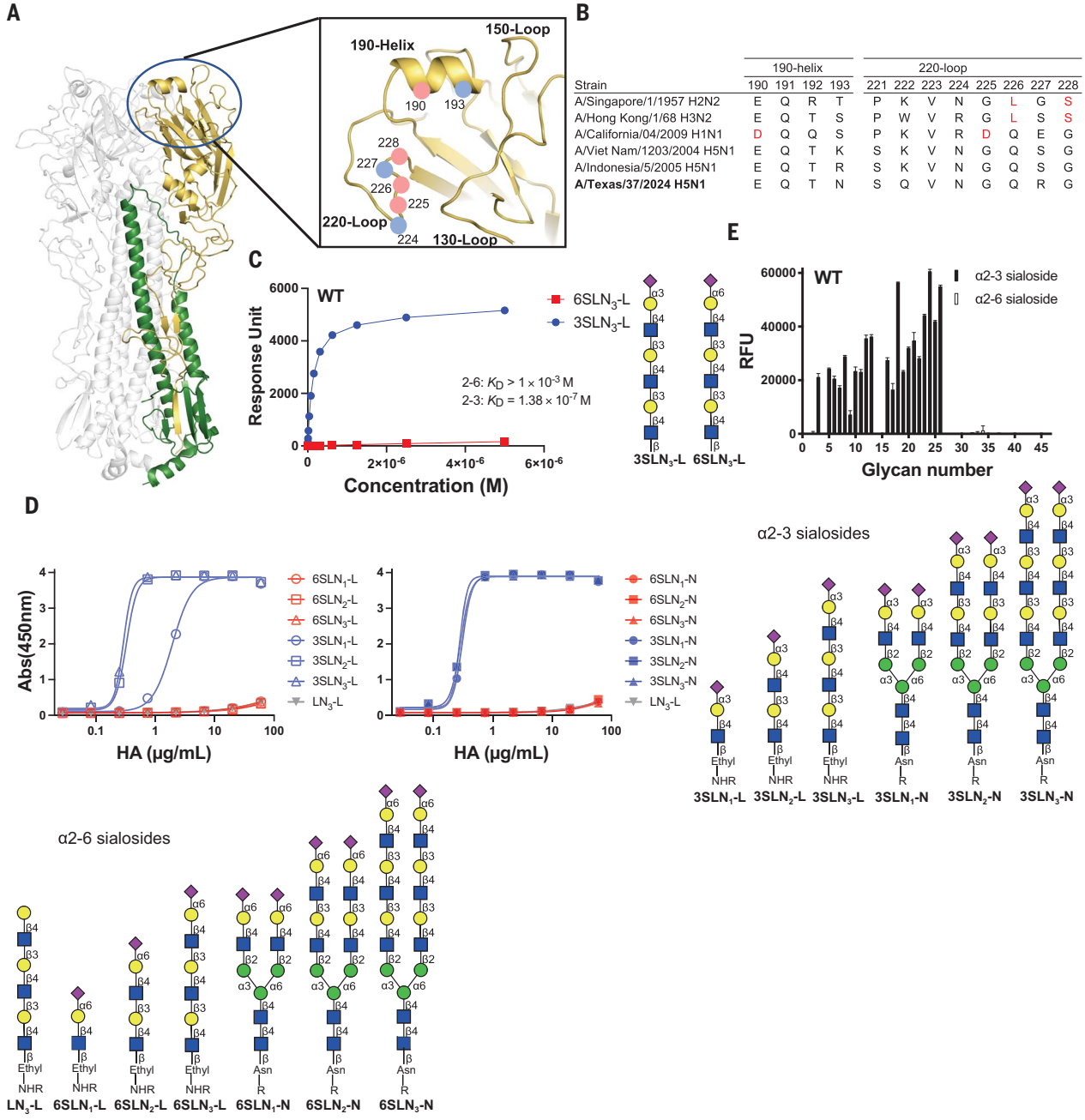

Fig. 1. Receptor characterization of WT bovine Texas H5 HA from A/Texas/37/2024 (H5N1). (**A**) The crystal structure of Apo Texas H5 HA was determined at 2.70-Å resolution (table S1). One HA monomer is highlighted in yellow for HA1 and in green for HA2. The receptor binding site is composed of the 130 loop, 150 loop, 190 helix, and 220 loop (see inset). Key residues and additional mutations analyzed in this study are shown as red and lavender dots, respectively. (**B**) Sequence comparison of 190 helix and 220 loop of WT Texas with human pandemic H1, H2, and H3 HA and human-infecting H5N1 HA. The hallmark residues for switch of receptor binding preference in H1, H2, and H3 are highlighted in red. (**C**) Binding affinity was measured by SPR. Response units are plotted against protein concentration. The binding curves representing α2-3 and α2-6 are blue and red, respectively. (**D**) The α2-3 and α2-6 sialosides in the ELISA are based on linear (left, open shapes) and biantennary (right, solid shapes) N-linked glycans, each with one to three repeats of LacNAc (Galβ1-4GlcNAc), as shown in the diagrams below. L, linear; N, N-linked; LN_3-L, a non-sialylated glycan; Abs, absorbance, R, -LCLC-Biotin. (**E**) Glycan microarray analysis of WT bovine Texas H5 HA. Two subsets of sialosides for α2-3 (glycan 3 to 26, black bar) and α2-6 (glycan 27 to 46, white bar) sialylated glycans imprinted on the chip are listed in table S2. RFU, relative fluorescence units. Single-letter abbreviations for the amino acid residues referenced throughout this paper are as follows: E, Glu; Q, Gln; R, Arg; T, Thr; P, Pro; S, Ser; D, Asp; G, Gly; N, Asn; K, Lys; W, Trp; V, Val; L, Leu; A, Ala; I, Ile.

binding of the $Gln^{226}Leu$ mutant HA to human-type receptors was weaker than the binding of the WT HA to α2-3 sialosides, the change in specificity was nevertheless clear and pronounced in all three assays. Moreover, in the ELISA, the Leu^{226} mutant bound more avidly to the α2-6 sialylated N-linked glycans than did the HA from the human 2009 H1N1 swine pandemic virus (A/California/04/2009, CA04) (Fig. 2B).

To create the Leu^{226}/Ser^{228} pairing that confers human-type receptor specificity in HAs of

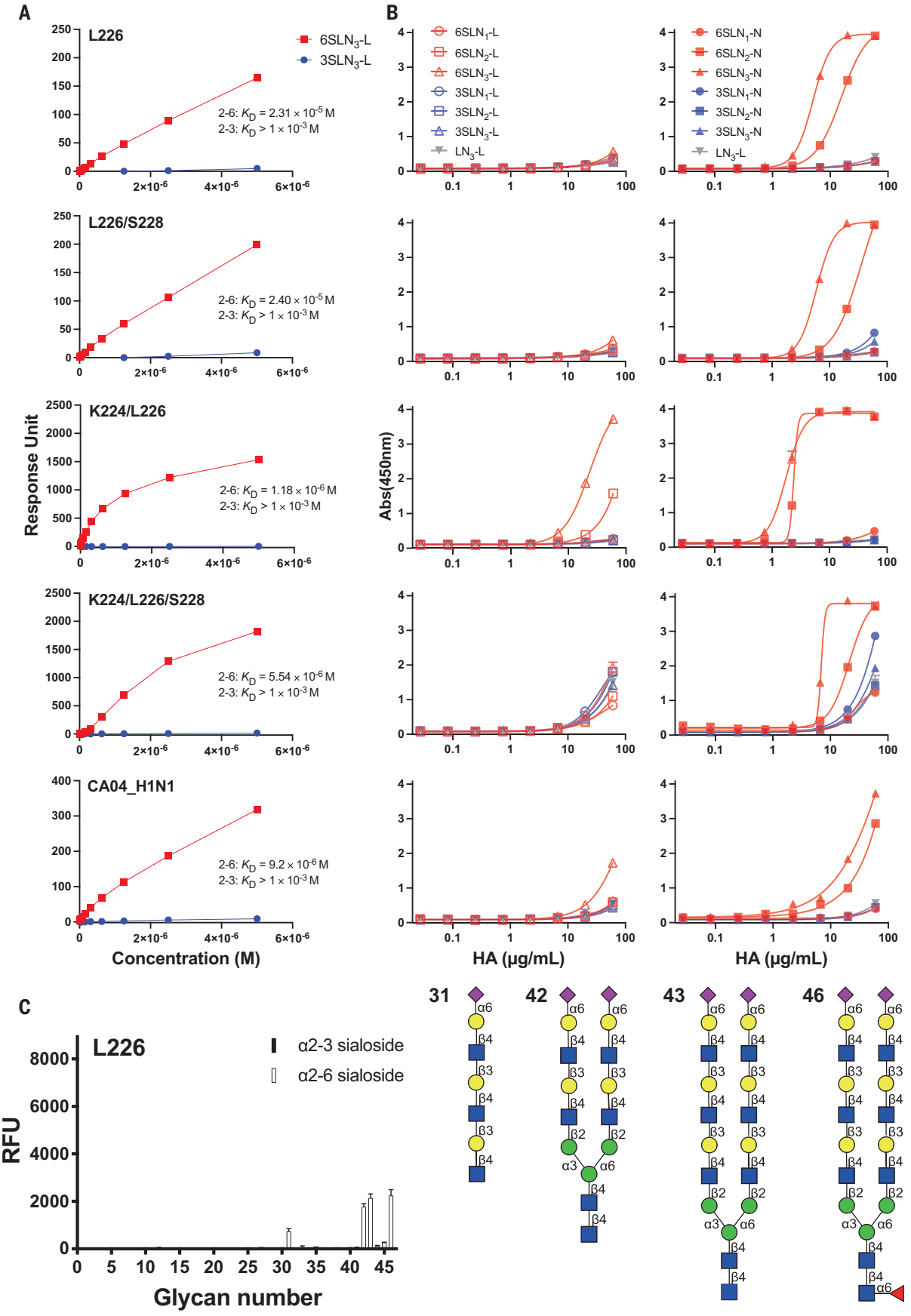

Fig. 2. Receptor specificity of bovine Texas H5 HA with a Gln^{226}Leu mutation and in combination with other mutations. The glycan receptor specificity for the H5 HA with Leu^{226}, Leu^{226}/Ser^{228}, Lys^{224}/Leu^{226}, and Lys^{224}/Leu^{226}/Ser^{228} mutations in the RBS were measured by SPR (**A**), ELISA (**B**), and glycan array (**C**). A/California/04/09 (CA04) H1 HA was used as a positive control for binding to α2-6 sialosides. (A) The K_D for each mutant in SPR assays was calculated based on the response units in figs. S1 and S2 using the Biacore S200 evaluation software static affinity model. (B) Extended linear (left) and biantennary (right) α2-3 and α2-6 sialosides were used in the ELISA. The schematic structures of the glycans are represented in Fig. 1. (C) Texas HA Leu^{226} mutant binding to the glycan array. Glycan numbers 3 to 26 on the array are for α2-3 sialosides (black bars), and 27 to 46 are for α2-6 sialosides (white bars). The schematic shows main glycan structures represented in the binding to α2-6 sialosides. Glycan numbers refer to the glycans shown in table S2.

H2N2 and H3N2 human viruses, we produced the Texas H5 HA with both the Gln^{226}Leu and Gly^{228}Ser mutations. This double mutant exhibited a specificity for α2-6 sialosides, similar to the mutant with Gln^{226}Leu alone (Fig. 2, A and B). However, substitution of Gly^{228}Ser alone abrogated binding to both α2-3 and α2-6 sialosides in SPR and ELISA (figs. S1 to S3). We also produced HAs with Glu^{190} to Asp^{190} or Gly^{225} to Asp^{225}, which are hallmark residues for the avian- to human-type switch in receptor binding in H1 pandemic viruses (*33*, *38*). These mutations either eliminated binding to α2-3 and α2-6 sialosides (Asp^{190}) or retained avian-type binding preference (Asp^{225}) (figs. S1 to S3), suggesting that they are not able to effect binding from avian- to human-type receptors in Texas H5 HA.

Some earlier investigations into the receptor specificity and transmission of H5N1 strains found that three HA mutations were required to effect a change to human-type receptor specificity (*45*, *49*, *50*). In one case, Asn^{224}Lys was paired with Gln^{226}Leu (*49*). When the Asn^{224}Lys mutation was introduced into the Texas HA with either Leu^{226} or Leu^{226}/Ser^{228}, binding to extended linear α2-6 sialosides by SPR and extended linear and biantennary N-linked α2-6 sialosides by ELISA was enhanced, particularly to Lys^{224}/Leu^{226} (Fig. 2, A and B). Weak binding to α2-3 sialosides was found in the Lys^{224}/Leu^{226}/Ser^{228} triple mutant in comparison to the Leu^{226}/Ser^{228} double mutant, which showed negligible binding to α2-3 sialosides (Fig. 2, A and B). We also combined the Leu^{226} mutant with other mutations, including Asn^{193}Thr, Asn^{193}Lys, Arg^{227}Asn, Arg^{227}Ser, and Arg^{227}Gln, which had previously shown improvement in H5 HA human-type receptor binding (*53*–*55*). However, none of these mutations exhibited notable increases in binding to α2-6 sialosides when combined with the Leu^{226} mutant and, indeed, generally also eliminated binding to α2-3 sialosides (figs. S1, S2, and S4). Binding of these mutants was predominantly to biantennary α2-6 sialosides (fig. S4). Taken together, these results indicate that the Leu^{226} substitution from Gln^{226} is key to a switch in avian- to human-type receptor preference in Texas H5 HA.

Crystal structure of Texas H5 HA with avian receptor analog LSTa

To assess the structural basis of how mutations switch the receptor specificity in the Texas H5 HA, we first determined a crystal structure at 2.32-Å resolution for WT Texas H5 HA with a natural sialo-pentasaccharide from human milk LSTa (Neu5Acα2-3Galβ1-3GlcNAcβ1-3Galβ1-4Glc, referred to below as Sia-1, Gal-2, GlcNac-3, Gal-4, and Glc-5) (Fig. 3A and table S1), which is an avian-type receptor analog (*56*). In the Texas H5 HA complex with LSTa, all five monosaccharide moieties are well ordered as indicated by clear, interpretable electron density (fig. S5, left), which may be impacted to some extent by a fortuitous crystal packing contact of the last monosaccharide moiety Glc-5 with a symmetry-related HA molecule (fig. S6). Structural comparisons were carried out for the LSTa complex of Texas H5 HA with H5N1 HA from A/Vietnam/1194/2004 [VN1194, clade 1, Protein Data Bank (PDB) ID 3ZP0] (*57*), which shares the same HA head domain with H5N1 HA from A/Vietnam/1203/2004 (Viet04, clade 1) (*57*) and H5N1 HA from A/Indonesia/5/2005 (Indo05, clade 2.1.3.2, PDB ID 4K63) (*43*) (Fig. 3, B to E). The Sia-1 (sialic acid) and Gal-2 (galactose) of LSTa bind to these three WT H5 HAs in a similar way, which contribute to specificity with avian-type receptors, where LSTa is in a trans conformation about the glycosidic bond between Gal-2 and Sia-1. The key avian H5 residue Gln^{226} makes hydrogen bonds with these two glycans (Fig. 3) (*42*). In VN1194 and Indo05 H5 HAs, the hydroxyl sidechain of Ser^{137} hydrogen bonds to the Sia-1 carboxyl group, whereas in Texas H5 HA, the Ala^{137} sidechain cannot form a hydrogen bond with LSTa (Fig. 3, A to C). The backbone carbonyl of Val^{135}, the backbone amide of residue 137, and the Glu^{190} carboxyl also hydrogen bond with Sia-1 in all three structures. The last three carbohydrate moieties, GlcNAc-3 (N-acetylglucosamine), Gal-4, and Glc-5 (glucose) of LSTa, exit the binding pocket and make weak or no direct interactions with Texas H5 HA (Fig. 3A); GlcNAc-3 was found to be shifted from the corresponding GlcNAc-3 in Indo05 H5 HA complex (Fig. 3E).

Crystal structure of Texas H5 HA Gln^{226}Leu with human receptor analog LSTc

The Texas H5 HA Gln^{226}Leu mutation alone was sufficient to switch the specificity from avian- to human-type receptors (Fig. 2 and figs. S1 and S2). We therefore determined the crystal structure at 2.7-Å resolution for Texas H5 HA Leu^{226} mutant with human-type receptor analog LSTc (Neu5Acα2-6Galβ1-4GlcNAcβ1-3Galβ1-4Glc), which is also a natural sialopentasaccharide from human milk (Fig. 4A and table S1). Similar to the LSTa complex with Texas H5 HA, all five monosaccharide moieties of LSTc could be modeled (fig. S5, right). By comparison, in the LSTc complex with ferret-transmissible mutants of Viet04 HA (PDB ID 4KDO) (*49*) (Fig. 4B) and Indo05 HA (PDB ID 4K67) (*43*) (Fig. 4C), only the first three monosaccharides could be modeled. However, the first four monosaccharides were modeled in the LSTc complex with a Gln^{226}Leu mutation of H5N1 HA (*E5.1*) from A/duck/Egypt/10185SS/2010 (dkEgy10, clade 2.2.1), which showed an avian- to human-type receptor specificity switch (*58*, *59*) (Fig. 4D), likewise LSTc in complex with human H2N2 HA from A/Singapore/1/1957 (Fig. 4E) (57H2, PDB ID 2WR7) (*60*).

Consistent with the α2-6 specificity and the crystal structures of these H5 mutants and H2 HAs, LSTc in the Leu^{226} mutant also adopts a cis conformation and binds Texas HA in a manner similar to dkEgy10 Q226L *E5.1* HA and 57H2 HA but distinct from that of Viet04 and Indo05 mutants, especially in the trajectory and orientation of GlcNAc-3 (Fig. 4). In all these HA-LSTc complexes, the conformation of Sia-1 and Gal-2 is similar, with Leu^{226} making van der Waals' contacts with the nonpolar portions of LSTc; however, Ala^{137} of bovine HA cannot make a sidechain hydrogen bond with Sia-1, unlike Ser^{137} in the other three H5 structures, although its main chain amide makes a hydrogen bond in all structures (Fig. 4). In the Leu^{226} mutant, Lys^{156} and Asn^{193} make additional hydrogen bonds to the Glc-5 moiety of LSTc, which contribute to binding of LSTc to the Texas H5 HA (Fig. 4A). Although Lys^{156} is conserved in the other three H5 HAs, Asn^{193} of Texas HA is not conserved, Lys^{193} is found in Viet04, and Arg^{193} is found in both Indo05 and dkEgy10 (Fig. 4). In another study, a Lys^{193}Thr mutation in ferret-transmissible Viet04 and Indo05 mutants enhanced human-type receptor binding (*53*). It is noteworthy that Lys^{222} makes a hydrogen bond with Gal-2 in dkEgy10 *E5.1* HA and 57H2 HA, although it is too distant to make such a hydrogen bond with Gal-2 in Viet04 and Indo05 HA mutants. In Texas HA, Gln^{222} makes no hydrogen bond to LSTc (Fig. 4).

In WT Viet04 and Indo05 H5 HAs, there is *N*-glycosylation of Asn^{158}, which is believed to reduce human-type receptor binding and was removed in the ferret-transmissible mutants

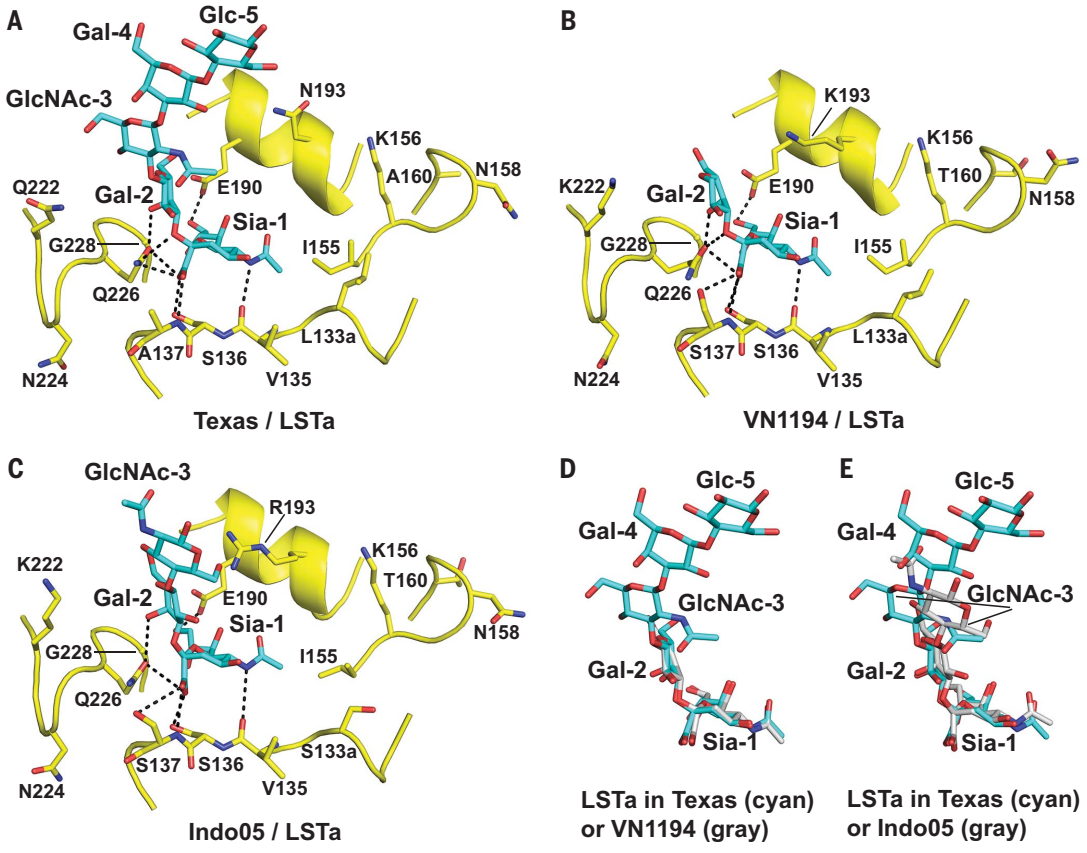

Fig. 3. Crystal structure of bovine Texas H5 HA with avian receptor analog LSTa and comparison with other H5 HA structures bound to LSTa. (**A**) RBS of WT Texas H5 HA (yellow carbon, blue nitrogen, and red oxygen atoms) bound with LSTa (cyan carbon, blue nitrogen, and red oxygen atoms). (**B**) RBS of VN1194 H5 HA bound with LSTa (PDB ID 3ZP0). (**C**) RBS of Indo05 H5 HA bound with LSTa (PDB ID 4K63). (**D**) Superposition of LSTa in Texas H5 HA and VN1194 H5 HA. (**E**) Superposition of LSTa in Texas H5 HA and Indo05 H5 HA. The HA structures are in a similar orientation after superimposition of their receptor binding subdomain (residues 117 to 265).

(*49*, *50*). However, since around 2005, the 158 *N*-glycosylation of H5 HAs is rare (*44*), which is the case in dkEgy10 and Texas H5 HAs (Fig. 4). Combining this critical feature with the shorter side chain of Asn^{193} (compared with Lys^{193} or Arg^{193}), which hydrogen bonds with Glc-5, may enable the trajectory of LSTc to move closer to the 190 helix and 150 loop (Fig. 4A).

It is also noteworthy that the Texas and Viet04 mutant HAs have a Leu^{133a} insertion, and the Indo05 mutant HA a Ser^{133a} insertion, whereas no 133a insertions are present in dkEgy10 and 57H2 HAs (Fig. 4). The role of the 133a insertion in receptor binding has been investigated in previous studies with dkEgy10 H5 HA, which showed that insertion of Ser^{133a} abrogates receptor binding to both avian- and human-type receptors (*58*, *59*), which is not the case for Texas H5 HA.

Conclusions

Whereas avian influenza H5N1 viruses impact the annual production of poultry and eggs, they also cause severe illness in marine and terrestrial mammals and pose a threat to human health owing to sporadic infections from domestic animals and the potential for the virus to emerge as a new pandemic strain in an immunologically naïve human population (*32*). Since 2021, H5 subtype clade 2.3.4.4b viruses have become a dominant strain in wild birds, poultry, and dairy cows and have infected other mammalian species, including terrestrial and marine mammals as well as humans (*13*). However, to date, mutations in the RBS of clade 2.3.4.4b H5 HA that switch to human-type receptor specificity have not been reported in the literature. Through glycan binding studies and x-ray structure determination of recombinant bovine H5 HA, we have shown that the bovine H5N1 clade 2.3.4.4b virus retains specificity for avian-type receptors. Several other reports have similarly concluded that the WT bovine H5N1 exhibits only avian-type receptor specificity by analyzing either recombinant HA produced in mammalian cells or the whole virus by using assays identical or similar to those used in this study (*51*, *52*, *61*). A $Thr^{199}Ile$ mutation in the HA of H5N1 viruses since 2023 was indeed reported to increase breadth to α2-3–linked avian-type receptors for Texas H5 HA (*62*). Another report evaluating intact virus with an assay using polymeric sialoside ligands concluded that the bovine H5N1 exhibited avian-type specificity with weaker specificity for human-type receptors (*63*). By using the same assay, the distantly related Viet04 H5N1 virus as a reference showed dominant binding to avian-type receptors and weak binding to human-type receptors (*63*). All reports agree that the bovine H5N1 virus retains predominantly avian-type receptor specificity.

A switch from avian- to human-type receptor specificity is considered a major risk factor for transmission in humans (*33*, *35*, *64*). For this reason, our observation that the single Texas H5 HA $Gln^{226}Leu$ mutation can switch receptor specificity is a clear concern. The bovine airway and mammary gland epithelium have predominantly avian-type and, to a lesser extent, human-type receptors (*65*, *66*), which provide little selective pressure for acquiring human-type receptor specificity. However, H5N1 infection of dairy workers, who have human-type receptors (*34*), provide selective pressure for human-type receptor specificity. Furthermore, in the flu season, coinfection with seasonal influenza viruses could lead to reassortment of bovine and human viruses and the creation of a hybrid virus that is more adapted for human infection.

Although the binding affinity of the $Gln^{226}Leu$ H5 HA mutant to the human-type receptors is relatively weak, the HAs of some human influenza viruses that have been able to transmit in the human population also exhibit weak

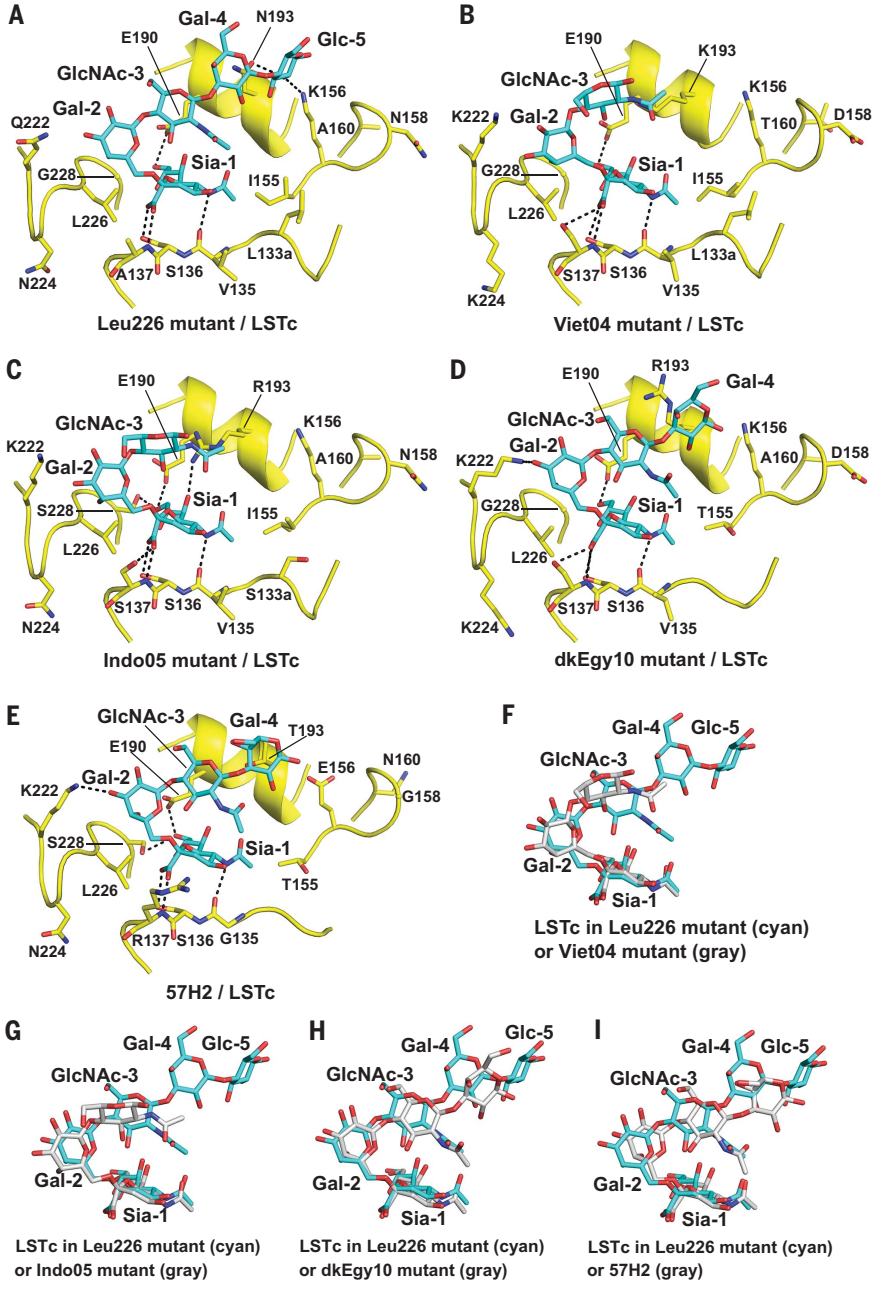

Fig. 4. Crystal structure of bovine Texas H5 HA Leu^{226} mutant with human receptor analog LSTc and comparison with other HA structures bound to LSTc. (**A**) RBS of Texas H5 HA Leu^{226} mutant (yellow carbon, blue nitrogen, and red oxygen atoms) bound to LSTc (cyan carbon, blue nitrogen, and red oxygen atoms). (**B**) RBS of Viet04 H5 HA ferret-transmissible mutant (Asn^{158}Asp/Asn^{224}Lys/Gln^{226}Leu/Thr^{318}Ile, H3 numbering) with LSTc (PDB ID 4KDO). (**C**) RBS of Indo05 H5 HA airborne ferret-transmissible mutant (His^{110}Tyr/Thr^{160}Ala/Gln^{226}Leu/Gly^{228}Ser, H3 numbering) with LSTc (PDB ID 4K67). (**D**) RBS of dkEgy10 H5 HA human receptor preference *E5.1* mutant (Gln^{226}Leu) with LSTc (PDB ID 5E30). (**E**) RBS of 57H2 HA with LSTc (PDB ID 2WR7). (**F**) Superposition of LSTc in Texas HA Leu^{226} mutant and in a Viet04 H5 HA ferret-transmissible mutant. (**G**) Superposition of LSTc in Texas HA Leu^{226} mutant and in the Indo05 H5 HA ferret-transmissible mutant. (**H**) Superposition of LSTc in Texas HA Leu^{226} mutant and dkEgy10 H5 HA human receptor preferring mutant. (**I**) Superposition of LSTc in Texas HA Leu^{226} mutant and 57H2 HA. The HA structures are in a similar orientation after superimposition of their receptor binding subdomain (residues 117 to 265).

binding to human-type receptors (*67*). In particular, the HA from the 2009 "swine flu" H1N1 pandemic virus CA04 exhibited even lower avidity to biantennary N-linked glycan receptors in the ELISA-based assay than the Leu^{226}-mutant H5 HA (Fig. 2B). The SPR data correspondingly showed weak binding of CA04 H1 HA for human-type receptors (Fig. 2A and fig. S2). With whole viruses, the relatively weak affinity observed with soluble HA trimers is amplified by the high density of HA molecules on the viral surface, affording increased avidity through simultaneous interactions with multiple receptors on the surface of the cell (*68*). Furthermore, with one additional mutation, Asn^{224}Lys, or two additional mutations, Asn^{224}Lys and Gly^{228}Ser, the bovine H5 HA mutants Asn^{224}Lys /Gln^{226}Leu and Asn^{224}Lys / Gln^{226}Leu/Gly^{228}Ser can bind more strongly to human-type receptors to achieve a level that is only slightly weaker than WT HA binding to avian-type receptors. Further studies are warranted for the phenotypic effects of such mutations to the H5N1 virus, such as virus entry, replication, and stability, among others (*47*). In addition to HA receptor specificity, other factors can affect transmission, such as a Glu^{627}Lys mutation in polymerase basic 2 (PB2) protein (*50*, *69*), and other human host factors, such as myxovirus resistance protein A (MxA), butyrophilin subfamily 3 member A3 (BTN3A3), and acidic nuclear phosphoprotein 32 (ANP32) (*70*), which are associated with viral adaptation in mammalian hosts and viral replication in human cells. Notably, Glu^{627}Lys in PB2 has been detected in the first human-infecting Texas virus (*26*); otherwise, the sequence of Texas HA is highly similar to that of other bovine H5 HAs from cows and infected humans, with a sequence identity of 99.5 to 100% (figs. S7 and S8).

Our structural analyses and binding assays provide insights into the bovine H5 HA receptor binding and mutations that can switch specificity from avian to human receptors. Notably, a single Gln^{226}Leu mutation can completely switch bovine H5 HA to human-type receptor specificity. In a recent deep mutational scanning study of a related avian H5N1 virus from A/American Wigeon/South Carolina/USDA-000345-001/2021, mutations at residue 226, including Leu^{226}, were observed to increase binding to engineered α2-6 versus α2-3 293 cells (*48*). However, previous studies with most of the earlier H5 strains found that three or more mutations in the HA were usually required to switch receptor preference to from avian to human type (*45*, *49*, *50*, *54*). Because each mutation is independent and the probability of achieving additional mutations decreases exponentially, our observation that a single mutation is sufficient to switch receptor specificity in the Texas HA dramatically increases the likelihood of achieving this

phenotype required for human transmission. In addition, mutations that could potentially affect receptor binding specificity have been found at RBS positions, including 135, 160, and 222, but they only occurred once, 13 times, and once, respectively, in 900 recent bovine H5 HA sequences (fig. S7). Thus, it is important to continue to monitor for signs of such changes in the currently circulating H5N1 viruses.

Limitations

In this study, we have not analyzed all the factors associated with human transmission of zoonotic influenza viruses. As discussed above, receptor specificity is a key factor, but not the only one required for human-to-human transmission of influenza viruses. The HA fusion pH is also important for transmission and HA stability (*49*). The pH of fusion of a recent HA from a bovine virus (A/dairy cattle/Texas/24-008749-001-original/2024) was determined to be 5.9, which is higher than that associated with efficient airborne transmission (pH < 5.5) (*49*, *71*). The neuraminidase NA also plays a key role in infection, as well as the HA/NA balance related to receptor binding by the HA and receptor destroying activity of the NA. (*72*, *73*).

REFERENCES AND NOTES

1. X. Xu, N. J. Subbarao, N. J. Cox, Y. Guo, *Virology* **261**, 15–19 (1999).
2. A. Fusaro *et al*., *Virus Evol.* **10**, veae027 (2024).
3. B. Olsen *et al*., *Science* **312**, 384–388 (2006).
4. A. Fusaro *et al*., *Nat. Commun.* **10**, 5310 (2019).
5. M. Engelsma, R. Heutink, F. Harders, E. A. Germeraad, N. Beerens, *Microbiol. Spectr.* **10**, e0249921 (2022).
6. S. Lin *et al*., *Virol. Sin.* **39**, 358–368 (2024).
7. G. J. Smith, R. O. Donis; World Health Organization/World Organisation for Animal Health/Food and Agriculture Organization (WHO/OIE/FAO) H5 Evolution Working Group, *Influenza Other Respir. Viruses* **9**, 271–276 (2015).
8. M. Sagong *et al*., *Transbound. Emerg. Dis.* **69**, e3255–e3260 (2022).
9. V. Caliendo *et al*., *Sci. Rep.* **12**, 11729 (2022).
10. S. N. Bevins *et al*., *Emerg. Infect. Dis.* **28**, 1006–1011 (2022).
11. S. Youk *et al*., *Virology* **587**, 109860 (2023).
12. E. J. Elsmo *et al*., *Emerg. Infect. Dis.* **29**, 2451–2460 (2023).
13. G. Graziosi, C. Lupini, E. Catelli, S. Carnaccini, *Animals (Basel)* **14**, 1372 (2024).
14. B. D. Cronk *et al*., *Emerg. Microbes Infect.* **12**, 2249554 (2023).
15. J. D. Brown *et al*., *Emerg. Infect. Dis.* **30**, 1271–1274 (2024).
16. M. Falchieri *et al*., *Emerg. Microbes Infect.* **13**, 2361792 (2024).
17. J. A. Pulit-Penaloza *et al*., *Emerg. Microbes Infect.* **13**, 2332667 (2024).
18. M. Agüero *et al*., *Euro Surveill.* **28**, 2300001 (2023).
19. S. J. Sillman, M. Drozd, D. Loy, S. P. Harris, *J. Comp. Pathol.* **205**, 17–23 (2023).
20. E. R. Burrough *et al*., *Emerg. Infect. Dis.* **30**, 1335–1343 (2024).
21. A. Bruno *et al*., *J. Travel Med.* **30**, taad032 (2023).
22. S. Lair *et al*., *Emerg. Infect. Dis.* **30**, 1133–1143 (2024).
23. M. Leguia *et al*., *Nat. Commun.* **14**, 5489 (2023).
24. P. I. Plaza, V. Gamarra-Toledo, J. Rodríguez Euguí, N. Rosciano, S. A. Lambertucci, *Travel Med. Infect. Dis.* **59**, 102712 (2024).
25. M. Uhart *et al*., bioRxiv (2024); https://www.biorxiv.org/content/10.1101/2024.05.31.596774v1.
26. T. M. Uyeki *et al*., *N. Engl. J. Med.* **390**, 2028–2029 (2024).
27. Centers for Disease Control and Prevention, Current H5N1 bird flu situation in dairy cows, 2024; https://www.cdc.gov/bird-flu/situation-summary/mammals.html.
28. L. C. Caserta *et al*., *Nature* **634**, 669–676 (2024).
29. Centers for Disease Control and Prevention, Technical report: June 2024 Highly pathogenic avian influenza A(H5N1) viruses (2024); https://www.cdc.gov/bird-flu/php/technical-report/h5n1-06052024.html.
30. Centers for Disease Control and Prevention, H5 bird flu: current situation, (2024); https://www.cdc.gov/bird-flu/situation-summary/index.html?CDC_AA_refVal=https%3A%2F%2Fwww.cdc.gov%2Fflu%2Favianflu%2Favian-flu-summary.htm.
31. C. C. Drehoff *et al*., *MMWR Morb. Mortal. Wkly. Rep.* **73**, 734–739 (2024).
32. World Health Organization, Cumulative number of confirmed human cases of avian influenza A(H5N1) reported to WHO (2024); https://www.who.int/publications/m/item/cumulative-number-of-confirmed-human-cases-for-avian-influenza-a(h5n1)-reported-to-who–2003-2024–27-september-2024.
33. T. M. Tumpey *et al*., *Science* **315**, 655–659 (2007).
34. K. Shinya *et al*., *Nature* **440**, 435–436 (2006).
35. N. J. Cox, S. C. Trock, S. A. Burke, *Curr. Top. Microbiol. Immunol.* **385**, 119–136 (2014).
36. A. Jayaraman *et al*., *PLOS ONE* **6**, e17616 (2011).
37. A. J. Thompson, J. C. Paulson, *J. Biol. Chem.* **296**, 100017 (2021).
38. L. Glaser *et al*., *J. Virol.* **79**, 11533–11536 (2005).
39. G. N. Rogers *et al*., *Nature* **304**, 76–78 (1983).
40. Y. Liu *et al*., *J. Virol.* **84**, 12069–12074 (2010).
41. A. H. Reid *et al*., *Emerg. Infect. Dis.* **9**, 1249–1253 (2003).
42. J. Stevens *et al*., *Science* **312**, 404–410 (2006).
43. W. Zhang *et al*., *Science* **340**, 1463–1467 (2013).
44. J. Stevens *et al*., *J. Mol. Biol.* **381**, 1382–1394 (2008).
45. J. C. Paulson, R. P. de Vries, *Virus Res.* **178**, 99–113 (2013).
46. S. Chutinimitkul *et al*., *J. Virol.* **84**, 6825–6833 (2010).
47. D. Eggink *et al*., *J. Virol.* **94**, e00195–e00120 (2020).
48. B. Dadonaite *et al*., *PLOS Biol* **22**, e3002916 (2024).
49. M. Imai *et al*., *Nature* **486**, 420–428 (2012).
50. S. Herfst *et al*., *Science* **336**, 1534–1541 (2012).
51. P. Chopra *et al*., bioRxiv (2024); https://www.biorxiv.org/content/10.1101/2024.07.30.605893v1.
52. J. J. S. Santos *et al*., bioRxiv (2024); https://www.biorxiv.org/content/10.1101/2024.08.01.606177v1.
53. W. Peng *et al*., *J. Virol.* **92**, e02016–e02017 (2018).
54. L. M. Chen *et al*., *Virology* **422**, 105–113 (2012).
55. R. P. de Vries *et al*., *PLOS Pathog.* **13**, e1006390 (2017).
56. M. B. Eisen, S. Sabesan, J. J. Skehel, D. C. Wiley, *Virology* **232**, 19–31 (1997).
57. M. Crusat *et al*., *Virology* **447**, 326–337 (2013).
58. K. Tharakaraman *et al*., *Cell* **153**, 1475–1485 (2013).
59. X. Zhu *et al*., *Cell Rep.* **13**, 1683–1691 (2015).
60. J. Liu *et al*., *Proc. Natl. Acad. Sci. U.S.A.* **106**, 17175–17180 (2009).
61. J. Yang *et al*., bioRxiv (2024); https://www.biorxiv.org/content/10.1101/2024.09.27.615407v1.
62. M. R. Good, W. Ji, M. L. Fernández-Quintero, A. B. Ward, J. J. Guthmiller, bioRxiv (2024); https://www.biorxiv.org/content/10.1101/2024.06.22.600211v1.
63. A. J. Eisfeld *et al*., *Nature* **633**, 426–432 (2024).
64. M. Imai, Y. Kawaoka, *Curr. Opin. Virol.* **2**, 160–167 (2012).
65. C. Kristensen, H. E. Jensen, R. Trebbien, R. J. Webby, L. E. Larsen, *Emerg. Infect. Dis.* **30**, 1907–1911 (2024).
66. R. K. Nelli *et al*., *Emerg. Infect. Dis.* **30**, 1361–1373 (2024).
67. R. Xu *et al*., *J. Virol.* **86**, 9221–9232 (2012).
68. A. Harris *et al*., *Proc. Natl. Acad. Sci. U.S.A.* **103**, 19123–19127 (2006).
69. H. Zhang *et al*., *J. Gen. Virol.* **95**, 779–786 (2014).
70. P. P. Petric, M. Schwemmle, L. Graf, *PLOS Pathog.* **19**, e1011450 (2023).
71. J. Yang *et al*., bioRxiv (2024); https://www.biorxiv.org/content/10.1101/2024.07.09.602706v1.
72. Y. Shtyrya *et al*., *Glycoconj. J.* **26**, 99–109 (2009).
73. N. Le Briand *et al*., *Virologie* **20**, 47–60 (2016).

ACKNOWLEDGMENTS

We thank H. Tien for helping with the automated robotic crystal screening at The Scripps Research Institute. **Funding:** This research was partially funded by National Institutes of Health NIAID Centers of Excellence for Influenza Research and Response contract 75N93021C00015 / PENN CEIRR (I.A.W. and J.C.P.). X-ray diffraction datasets were collected at the Stanford Synchrotron Radiation Lightsource (SSRL) beamlines 12-1 and 12-2 and the National Synchrotron Light Source II (NSLS II) beamline 17-ID-2. Use of the SSRL, SLAC National Accelerator Laboratory, is supported by the US Department of Energy (DOE), Office of Science, Office of Basic Energy Sciences under contract no. DE-AC02-76SF00515. The SSRL Structural Molecular Biology Program is supported by the DOE Office of Biological and Environmental Research and by the National Institutes of Health, National Institute of General Medical Sciences (P30GM133894). The contents of this publication are solely the responsibility of the authors and do not necessarily represent the official views of NIGMS or NIH. This research used resources of the National Synchrotron Light Source II, a US DOE Office of Science User Facility operated for the DOE Office of Science by Brookhaven National Laboratory under contract no. DE-SC0012704. **Author contributions:** T.-H.L., X.Z., J.C.P., and I.A.W. conceived experiments. T.-H.L., W.Y., and S.B. prepared recombinant proteins. T.-H.L. and X.Z. acquired and analyzed x-ray data, D.Z. and T.-H.L. performed SPR experiments, S.W. performed ELISA experiments, S.W. prepared glycans for SPR and ELISA assays, and R.M. performed glycan array studies. T.-H.L., X.Z., J.C.P., and I.A.W. wrote the original manuscript. All authors reviewed and edited the manuscript. **Competing interests:** The authors declare that they have no competing interests. **Data and materials availability:** The x-ray coordinates and structure factors have been deposited in the Research Collaboratory for Structural Bioinformatics (RCSB) PDB under accession codes 9DIQ for Texas apo-HA, 9DIP for Texas HA with LSTa, and 9DIO for Texas HA Q226L mutant with LSTc.

SUPPLEMENTARY MATERIALS

science.org/doi/10.1126/science.adt0180
Materials and Methods
Figs. S1 to S8
Tables S1 and S2
References (*74*–*84*)
MDAR Reproducibility Checklist

Submitted 7 September 2024; accepted 4 November 2024
10.1126/science.adt0180

Correction (5 December 2024): In the print abstract, there is an error in two places: "Glu226Leu" should be "Gln226Leu." This was corrected in the PDF and XML but was not caught soon enough to correct in print. This correction is to alert readers to the print error.